Impact of Intracranial Aneurysm Morphology and Rupture Status on the Particle Residence Time

E.L. Leemans, B.M.W. Cornelissen, G. Rosalini, D. Verbaan, J.J. Schneiders, R. van den Berg, W.P. Vandertop, E.T. van Bavel, C.H. Slump, C.B.L.M. Majoie, H.A. Marquering

From the Department of Biomedical Engineering and Physics, Amsterdam UMC, University of Amsterdam, Amsterdam, the Netherlands (ELL, BMWC, GR, ETVB, HAM); Department of Radiology and Nuclear Medicine, Amsterdam UMC, University of Amsterdam, Amsterdam, the Netherlands (ELL, BMWC, JJS, RVDB, CBLMM, HAM); MIRA Institute for Biomedical Engineering and Technical Medicine, University of Twente, Enschede, the Netherlands (BMWC, CHS); Department of Industrial Engineering and Information, University of Pavia, Pavia, Italy (GR); and Neurosurgical Center Amsterdam, Amsterdam UMC, University of Amsterdam, Amsterdam, the Netherlands (DV, WPV).

ABSTRACT

BACKGROUND AND PURPOSE: **Aneurysm hemodynamics play an important role in aneurysm growth and subsequent rupture. Within the available hemodynamic characteristics, particle residence time (PRT) is relatively unexplored. However, some studies have shown that PRT is related to thrombus formation and inflammation. The goal of this study is to evaluate the association between PRT and aneurysm rupture and morphology.**

METHODS: **We determined the PRT for 113 aneurysms (61 unruptured, 53 ruptured) based on computational fluid dynamic models. Virtual particles were injected into the parent vessel and followed during multiple cardiac cycles. PRT was defined as the time needed for 99% of the particles that entered an aneurysm to leave the aneurysm. Subsequently, we evaluated the association between PRT, rupture, and morphology (aneurysm type, presence of blebs, or multiple lobulations).**

RESULTS: **PRT showed no significant difference between unruptured (1.1 seconds interquartile range [IQR .39-2.0 seconds]) and ruptured aneurysms (1.2 seconds [IQR .47-2.3 seconds]). PRT was influenced by aneurysm morphology. Longer PRTs were seen in bifurcation aneurysms (1.3 seconds [IQR .54-2.4 seconds], $P = .01$) and aneurysms with blebs or multiple lobulations (1.92 seconds [IQR .94-2.8 seconds], $P < .001$). Four of five partially thrombosed aneurysms had a long residence time (>1.9 seconds).**

CONCLUSIONS: **Our study shows an influence of aneurysm morphology on PRT. Nevertheless, it suggests that PRT cannot be used to differentiate unruptured and ruptured aneurysms.**

Keywords: Aneurysm, hemodynamics, blood flow, hemorrhage, morphology.

Acceptance: Received January 11, 2019, and in revised form March 29, 2019. Accepted for publication April 2, 2019.

Correspondence: Address correspondence to Eva L. Leemans, Departments of Biomedical Engineering and Physics, Radiology and Nuclear Medicine, Amsterdam UMC, University of Amsterdam, Room L0-104, Academic Medical Center, Meibergdreef 9, 1105AZ Amsterdam, the Netherlands. E-mail: e.l.leemans@amc.uva.nl

Acknowledgments and disclosure: This study was supported by a grant from the Toegepast Wetenschappelijk Instituut voor Neuromodulatie (TWIN association), Hengelo, the Netherlands. René van den Berg—UNRELATED: Consultancy: Codman Depuy Neurovascular, Comments: coil development,* Henk A. Marquering—OTHER RELATIONSHIPS: cofounder and shareholder of Nico-lab. Charles B.L.M. Majoie—RELATED: Grant: TWIN Foundation*; UNRELATED: Grants/Grants Pending: Dutch Heart Foundation, European Commission, Stryker.* OTHER RELATIONSHIPS: shareholder of Nico-lab *Money paid to the institution.

J Neuroimaging 2019;29:487-492.
DOI: 10.1111/jon.12618

Introduction

As patients with ruptured intracranial aneurysms have a high case fatality, preventive treatment of unruptured intracranial aneurysms is often considered.[1] However, both surgical and endovascular interventions may cause considerable complications, such as vessel perforation and thromboembolic stroke.[2,3] Thus, a need exists to accurately determine the actual rupture risk to decide which unruptured aneurysms should be treated. Currently, the rupture risk is based on morphological indices and patient characteristics such as size, shape, location, age, hypertension, and a history of subarachnoid hemorrhage.[4,5] These variables are combined into the PHASES score, which calculates the 5-year rupture risk. As a result, many small aneurysms and aneurysms in the anterior circulation remain untreated.[6] Several studies, however, have shown that a large percentage (~60%) of the ruptured aneurysms are small (<7 mm). Therefore, additional parameters are needed to further improve rupture risk prediction.[4,7]

Hemodynamics play an important role in the development, growth, and subsequent rupture of an aneurysm, and are frequently studied with computational fluid dynamics (CFD), which determines velocity and pressure using computer simulations.[8] Various hemodynamic parameters have been extensively studied, such as the wall shear stress (WSS) and oscillatory shear index (OSI).[5,9,10] Pathologic flow conditions–either high or low wall shear stress–lead to degenerative wall remodeling and inflammation.[11,12] However, the exact mechanisms are still unclear.

Another way to quantify hemodynamics inside aneurysms is the particle residence time (PRT), which can be acquired

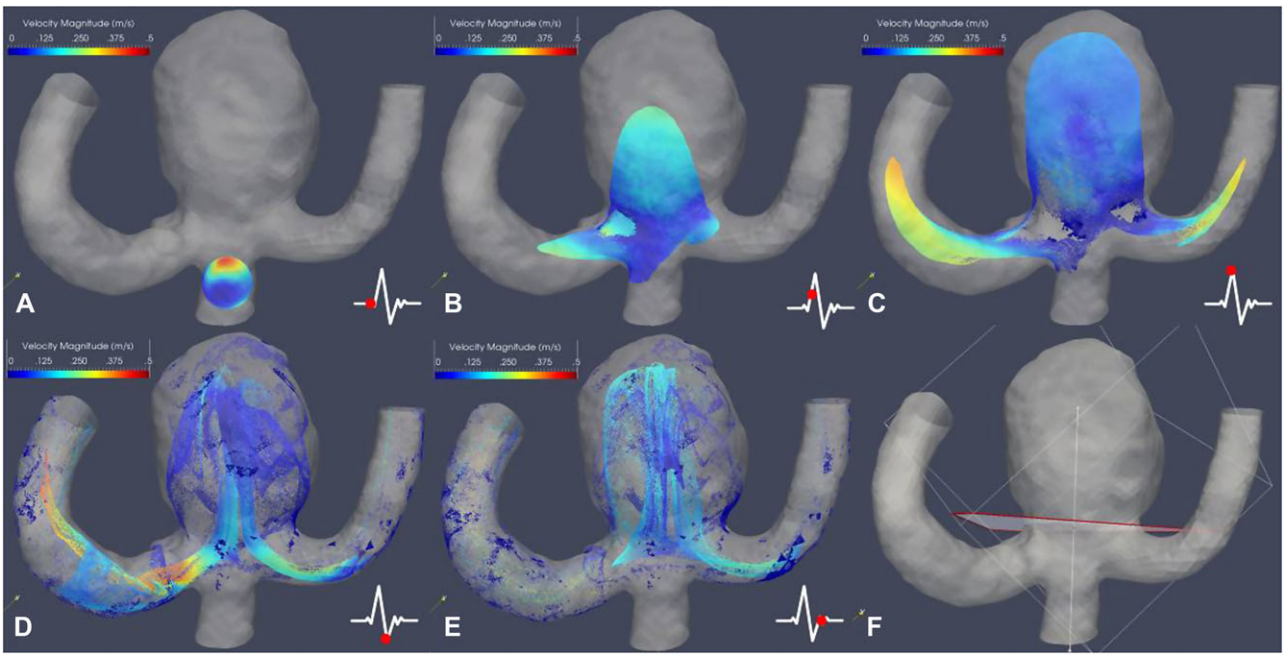

Fig 1. Particle tracking. (A) Spherical Point Source placed in the parent vessel containing 1,000,000 particles. (B) The inflow of particles in the aneurysm and (C) continuing until the top of the dome. (D) Multiple-vortexes distribute in the aneurysm region. (E) Most particles entered the normal vasculature but a proportion is trapped in the intra-aneurysmal vortices and (F) the aneurysm region gradually empties. The red dot on the electrocardiogram-signal in the bottom right corner marks the approximate time of the snapshot.

through postprocessing of CFD data.[13] The PRT reflects the time blood spends inside a specific region, such as an aneurysm. It has been shown that an increased PRT is associated with thrombus formation.[14,15] Longer PRTs likely result in aneurysm instability as it facilitates the activation of inflammatory cells and leukocyte transmigration into the aneurysm wall.[8,16,17] Hereby, the PRT influences the balance between repair and degradation of the aneurysm wall. However, it is unclear whether there is an association between PRT and rupture. We therefore evaluated the association between PRT, rupture, and aneurysm morphology in a prospectively collected cohort of ruptured and unruptured intracranial aneurysms.

Methods

Patients and CFD Data

This study used the CFD data set of the HEROICA study.[10] This study evaluated 102 patients with 117 saccular intracranial aneurysms, both ruptured ($n = 55$ [47%]) and unruptured ($n = 62$ [53%]). The study was approved by the institutional review board and written informed consent was obtained from all patients. Three aneurysms (one unruptured and two ruptured) were excluded because CFD data were missing or incomplete. The ruptured aneurysms were identified by the presence and location of the subarachnoid hemorrhage on admission Computed Tomography (CT). In 6 patients with multiple aneurysms, two experienced neuroradiologists (C.B.L.M.M. and R.v.d.B) inspected all clinical and radiologic data to select the most likely source of hemorrhage. The other aneurysms were classified as unruptured.

All patients underwent 3D rotational angiography (3DRA) as part of the standard clinical workup. These 3DRAs were used to segment the aneurysm and parent vasculature and create a mesh with tetrahedral elements. Segmentation was done semi-automatically using a level-set method and manual correction. Additionally, the neck size was reviewed by two neuroradiologists. Subsequently, CFD was performed for intra-aneurysmal flow calculations. Patient-specific velocity profiles obtained with Phase Contrast MR were used as inflow boundary condition, and the inflow profiles for specific locations can be seen in previous work.[18] Zero pressure boundary conditions were prescribed at all outlets. Blood was assumed to have an attenuation of 1,040 kg/m^3 and a dynamic viscosity of .004 Pa/seconds. Three cardiac cycles were simulated, but only the third complete cycle was used. All simulations were performed with Fluent (Ansys, Canonsburg, PA).

PRT Calculation

We defined PRT as the time needed for 99% of the particles that entered the aneurysm to leave the aneurysm. This number is selected as slower particles are more likely to cause alterations to the vessel wall and thrombus formation. To acquire this number, we simulated the particle tracks over time. First, the CFD velocity fields were imported into ParaView 5.1.2 (Kitware, Clifton Park, NY). To acquire a high temporal resolution, linear temporal interpolation was done with an interval of .01 second. Hereby, the particles could be tracked more accurately. A spherical source containing one million massless fluid particles was positioned in the inflow parent vessel of the aneurysm, see Figure 1A. The radius of this sphere was equal to the inflow vessel radius. For each interpolated time-step, the location of the particles was calculated through Lagrangian particle tracking using the particle tracer filter available in ParaView. Particles were tracked for at least four cardiac cycles. An example of the tracking is shown in Figure 1. The resulting data contain the position of all particles at each time-step, see Figure 2.

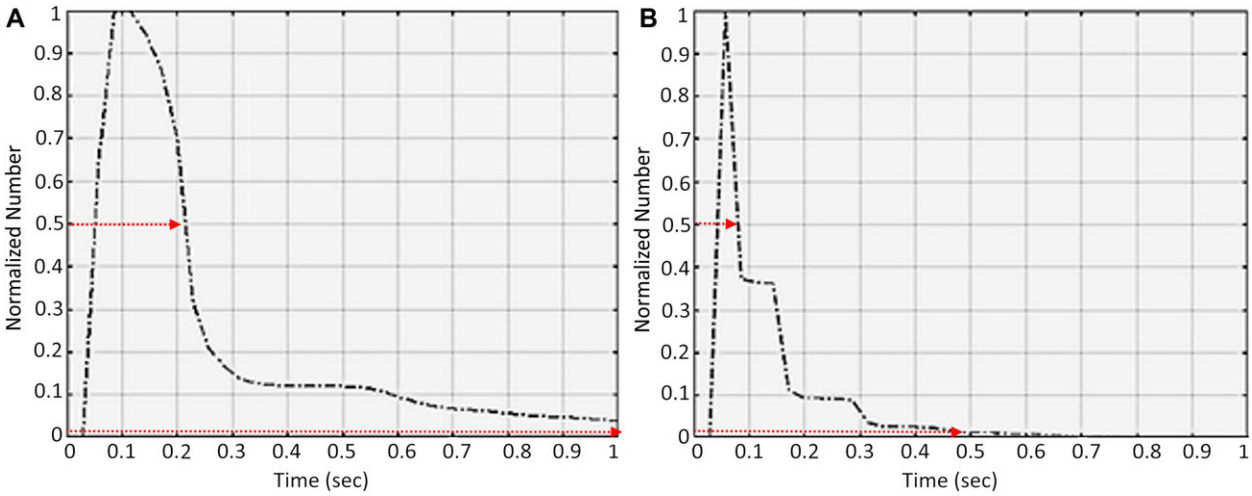

Fig 2. Normalized number of particles at each time-step during one cardiac cycle. The first dotted red line shows the particle half-life, and the second dotted red line shows the selected value for the particle residence time. The left plot shows data of a ruptured aneurysm, and the right plot shows data of an unruptured aneurysm.

We isolated the aneurysm from the vasculature to evaluate whether a particle was inside the aneurysm by positioning a plane at the aneurysm neck and cutting the 3D model along this plane (G.R.). The position of the neck plane was checked by a second observer (E.L.). In case of disagreement, the final neck plane was selected in consensus.

The position of all the particles at each time-step and the location of the aneurysm volume were imported into Matlab 2016a (Mathworks, Natick, MA). Subsequently, we calculated the number of particles within the aneurysm at each time step.

Statistical Analysis

Patient characteristics were expressed as mean ± standard deviation for normal distributions. Non-normally distributed variables were expressed as median and interquartile range (IQR, 25-75%). Normality of the data was tested using a one sample Shapiro-Wilk test.

The association between rupture status and PRT and conventional rupture risk determinants–namely, type, age, high-risk location (based on the phases score[6]), multiple lobulations, maximum diameter–was evaluated using univariable logistic regression analysis.

Differences in PRT between aneurysm configurations were tested using a *T*-test in case of normal distribution and a Mann-Whitney U test in case of a non-normal distribution. We compared bifurcation versus sidewall aneurysms and aneurysms with versus without blebs or multiple lobulations. Additionally, a Spearmen's rank correlation was done to determine the relationship between OSI, average and maximum WSS and PRT.

A *P*-value smaller than .05 was considered statistically significant. All analyses were performed by using the SPSS version 24, (IBM, Armonk, NY).

Results

This study included 99 patients (61 [54%] women) with 114 aneurysms. The mean age was 54.9 ± 12.0 years. Although a trend was seen toward more ruptured aneurysms at the communicating and posterior arteries, no significant differences were found ($P = .08$), see Table 1. In 13 (11%) of the 114 aneurysms, more than four cycles were needed for 99% of the particles to leave the aneurysm and in 10 of these cases, more than six cycles were needed. The median PRT for the total population was 1.19 seconds (IQR: .41-2.21).

Association of PRT with Rupture Status

Median PRT was 1.14 seconds (IQR: .39-2.04) and 1.20 seconds (IQR: .47-2.31) for unruptured and ruptured aneurysms, respectively. No significant difference was seen in PRT between unruptured and ruptured aneurysms, $P = .79$. The distribution of the PRT for both groups is displayed in Figure 3A. As shown in Table 1, only the presence of blebs or multiple lobulations was significantly associated with rupture status $P < .05$.

The correlation between PRT and OSI was not significant (.17, $P = .07$). However, a significant negative correlation was seen between PRT and WSS (−.47 and −.28, $P < .001$ and $P = .002$ for average and maximum WSS, respectively).

Association of PRT with Morphology

As shown in Figures 3B and C, PRT is influenced by aneurysm morphology. PRT is significantly longer in bifurcation 1.27 seconds (IQR: .54-2.40) compared to sidewall aneurysms .49 seconds (IQR: .14-1.62), $P = .01$ (Fig 3B). A significantly longer PRT was also seen in aneurysms with blebs or multiple lobulations: 1.92 seconds (IQR: .94-2.75) versus .82 seconds (IQR: .25-1.42) in regular aneurysms, $P < .001$ (Fig 3C). The PRT inside the bleb–the time it takes for 99% of the particles that entered the bleb to leave again–was .5-10 seconds. Figure 4 shows the remaining particles within an aneurysm with multiple blebs after four cardiac cycles. In this aneurysm, most particles that remain are inside one of the blebs. Five aneurysms were partially thrombosed (two ruptured), including four sidewall aneurysms and one bifurcation aneurysm. Four out of five thrombosed aneurysms had a long PRT (>1.9 seconds).

Discussion

We found no significant association between the PRT and rupture status. However, PRT was associated with aneurysm morphology. Longer PRTs were seen in bifurcation aneurysms, aneurysms with blebs or multiple lobulations, and partially thrombosed aneurysms.

Table 1. Univariable Analysis for the Relation Between PRT and Conventional Risk Factors and Rupture Status

Characteristic	Unruptured $N = 61$	Ruptured $N = 53$	Univariable	
			Odds ratio (95% CI)	*P*-value
PRT (second) Median (IQR)	1.1 (.39-2.0)	1.2 (.47-2.3)	1.03 (.81-1.32)	.79
Age (years)	55 ± 11	55 ± 13	1.01 (.98-1.04)	.70
Location:				
ICA	12 (20%)	8 (15%)	Ref	
MCA	27 (44%)	8 (15%)	.44 (.14-1.47)	.18
AcomA/PcomA/Posterior	22 (36%)	37 (70%)	2.52 (.89-7.12)	.08
Presence of blebs or multiple lobulations	17 (28%)	23 (46%)	2.21 (1.00-4.85)	.05
Size (mm) Median (IQR)	6.6 (4.6-9.1)	6.4 (4.3-7.9)	.93 (.83-1.05)	.26
Aneurysm type (bifurcation)	39 (64%)	41(77%)	.52 (.23-1.19)	.12

Abbreviations: *N* = number; IQR = interquartile range; ref = reference; PRT = particle residence time; ICA = internal carotid artery; MCA = middle cerebral artery; AcomA = anterior communicating artery; PcomA = posterior communicating artery.

In this study, both PRT and the conventional risk factors (age, size, and location)[6] showed no significant association with rupture status. Our study created the CFD-models based on 3DRA. In patients with ruptured aneurysms, 3DRA was part of standardized clinical workflow, while for patients with unruptured aneurysms 3DRA was only done when treatment was considered. Therefore, a selection bias is present as treatment is only considered in patients with a higher rupture risk, based on conventional criteria such as size and location. A prospective trial is needed to examine the relation between PRT and rupture more thoroughly.

A relation between flow conditions and rupture has been shown in several studies,[5,19,20] as pathologic flow conditions lead to degenerative wall remodeling and inflammation.[11,12] However, recent studies showed that degeneration and inflammation occur in both high and low flow conditions.[8,21] Therefore, the relation between PRT and rupture might not be straightforward. Flow stagnation could lead to thrombus formation and a hypertrophic vessel wall.[14,22] This might reflect ongoing repair, reducing the risk of rupture.

We observed significant longer residence times in aneurysms with blebs or multiple lobulations. This finding is in line with the study of Epshtein and Korin, who show that particles linger in the aneurysm vortex and stasis regions.[23] A slower flow is often present within the bleb or lobulation, resulting in higher PRT. Previous studies showed that bleb formation occurs at regions of high wall shear stress, but that the resulting bleb has a thin degenerated wall and a low wall shear stress.[24,25]

A long residence time likely gives inflammatory cells more time to adhere to the wall. This assumption could be explored by simulating monocyte deposition as proposed by Hardman et al, who developed a method for abdominal aortic aneurysms.[16] The method combines particle tracking and a model for macrophage adhesion to the wall to find hotspots of monocyte deposition. The model could be adapted to match the intracranial aneurysm pathology. Concurrently, such simulated regions of monocyte deposition can be correlated to other imaging markers such as vessel wall thickness,[26] wall enhancement, or histology.[27] Combining these parameters with the PRT will further improve our understanding of growth and rupture.

In line with previous studies,[14,15] our study showed a prolonged PRT in the lumen of partially thrombosed aneurysms. Based on our data, it cannot be concluded that PRT contributes to thrombus growth and development as we only looked at a single snapshot in time and only included a few patients with partially thrombosed aneurysms. However, this finding supports the assumption that PRT is closely related to thrombus formation.

Our study also showed a significant longer PRT in bifurcation aneurysms compared to sidewall aneurysms. A previous study also reported differences between bifurcation and sidewall aneurysms when examining maximum diameter, size ratio, inflow angle, and nonsphericity index.[28] Both findings indicate that bifurcation aneurysm varies from sidewall aneurysms in shape and hemodynamics. As a consequence, the process of growth and subsequently rupture may differ between these aneurysm types. However, aneurysm type was not significantly associated with rupture status in our analysis.

The used method for the calculation of PRT has limitations. Tambasco and Steinman showed that the quality of Lagrangian particle tracking also depends on the used mesh elements.[29] They have proposed to use adaptive meshes with small near wall elements. In our CFD-models, we did use a boundary layer with small elements near the vessel wall. However, the mesh might need further improvement especially in the regions with complex flow patterns.

This study used a single injection of particles in the parent vessel. With this method, we were able to track the general patterns within the aneurysm and the intra-aneurysmal vortices. However, the overall PRT might be even longer as tracking near the wall can be challenging due to the slow velocities in these areas. Furthermore, aneurysms often have a chaotic flow pattern,[30] with changing flow directions during the cardiac cycle. Continuous injection compensates for the differences in flow patterns during the cardiac cycle. Additionally, other tracking methods might improve the accuracy of the particle tracking;[30,31] however, these more sophisticated methods also have higher computational times which limits clinical implementation.

To determine the PRT, we selected a threshold, therefore the PRT reflects the slowest 1% of particles. This number is selected as slower particles likely cause alterations to the vessel wall. However, we did not test for the effect of other thresholds on the results. We did see that the half-life of particles inside the aneurysm (the time it takes for 50% to leave the aneurysm) was very fast and only small differences could be seen between aneurysms. Lowering the threshold might therefore reduce the differences between the analyzed aneurysms.

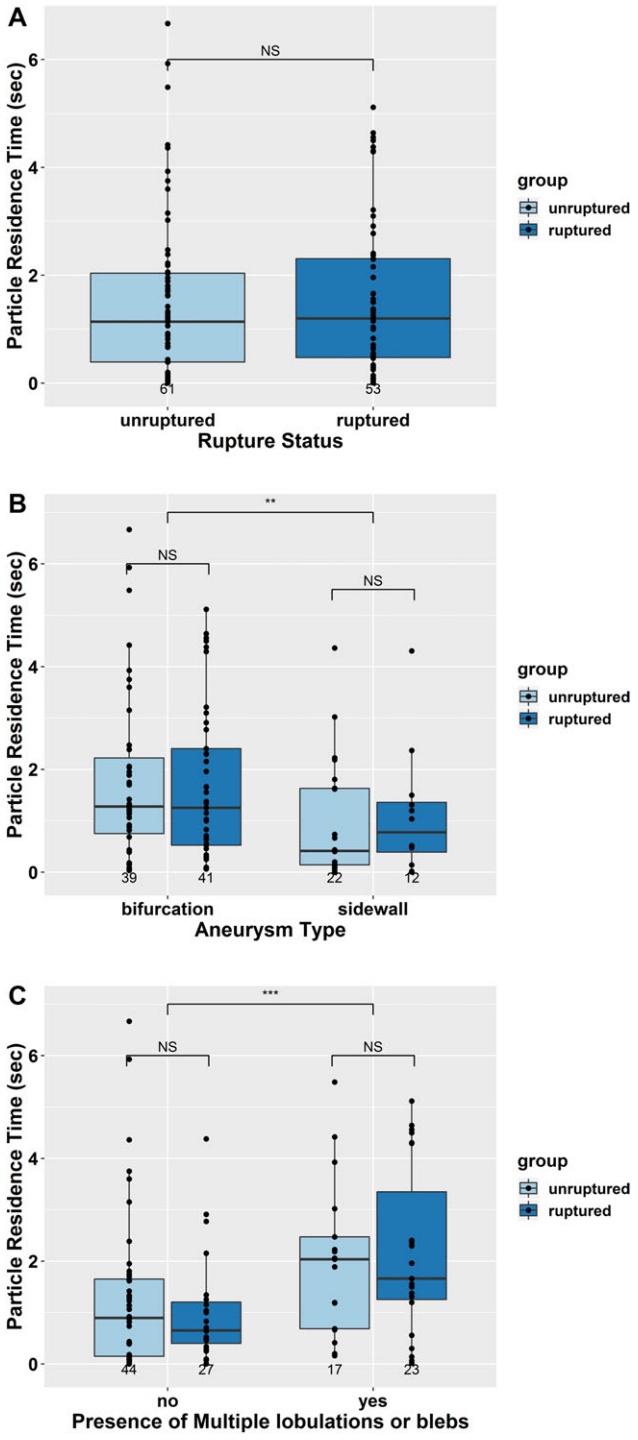

Fig 3. (A) Distribution of particle residence time (PRT) per rupture status, the large dots represent individual cases. (B) Distribution of PRT per aneurysm type and rupture status, the large dots represent individual cases. (C) Distribution of PRT for aneurysms with and without blebs or multiple lobulations and rupture status. The large dots represent individual cases. ** = significant difference ($P = .01$) *** = significant difference ($P < .001$).

To conclude, in our population, there was no significant association between PRT and rupture status. However, PRT was influenced by aneurysm morphology as longer residence times were seen in bifurcation aneurysms, aneurysms with blebs or multiple lobulations, and partially thrombosed aneurysms. Further research should focus on determining the PRT in a prospective cohort, focusing on the association between PRT and growth and rupture. Such a prospective trial helps to elucidate the usability of PRT to predict growth and rupture.

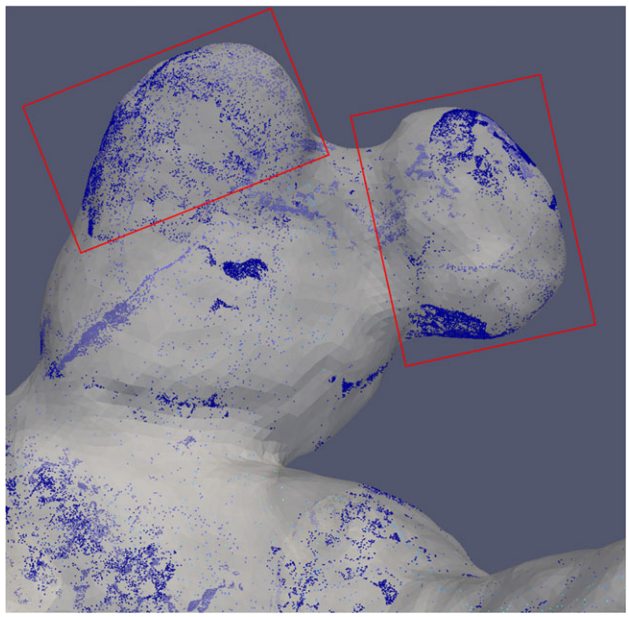

Fig 4. Distribution of particles after four cardiac cycles within an aneurysm with two blebs (red squares).

References

1. van Gijn J, Kerr RS, Rinkel GJ. Subarachnoid haemorrhage. Lancet 2007;369:306-18.
2. Zijlstra IJA, Verbaan D, Majoie CB, et al. Coiling and clipping of middle cerebral artery aneurysms: a systematic review on clinical and imaging outcome. J Neurointerv Surg 2016;8:24-9.
3. Ruan C, Long H, Sun H, et al. Endovascular coiling vs. surgical clipping for unruptured intracranial aneurysm: a meta-analysis. Br J Neurosurg 2015;29:485-92.
4. Raghavan ML, Ma B, Harbaugh RE. Quantified aneurysm shape and rupture risk. J Neurosurg 2005;102:355-62.
5. Cebral JR, Castro M, Burgess JE, et al. Characterization of cerebral aneurysms for assessing risk of rupture by using patient-specific computational hemodynamics models. Am J Neuroradiol 2005;26:2550-9.
6. Greving JP, Wermer MJH, Brown RD, et al. Development of the PHASES score for prediction of risk of rupture of intracranial aneurysms: a pooled analysis of six prospective cohort studies. Lancet Neurol 2014;13:59-66.
7. Weir B, Disney L, Karrison T. Sizes of ruptured and unruptured aneurysms in relation to their sites and the ages of patients. J Neurosurg 2002;96:64-70.
8. Meng H, Tutino VM, Xiang J, et al. High WSS or low WSS? Complex interactions of hemodynamics with intracranial aneurysm initiation, growth, and rupture: toward a unifying hypothesis. Am J Neuroradiol 2014;35:1254-62.
9. Castro MA, Putman CM, Sheridan MJ, et al. Hemodynamic patterns of anterior communicating artery aneurysms: a possible association with rupture. Am J Neuroradiol 2009;30:297-302.
10. Schneiders JJ, Marquering HA, van Ooij P, et al. Additional value of intra-aneurysmal hemodynamics in discriminating ruptured versus unruptured intracranial aneurysms. Am J Neuroradiol 2015;36:1920-6.
11. Laaksamo E, Ramachandran M, Frösen J, et al. Intracellular signaling pathways and size, shape, and rupture history of human intracranial aneurysms. Neurosurgery 2012;70:1565-72.

12. Chalouhi N, Ali MS, Jabbour PM, et al. Biology of intracranial aneurysms: role of inflammation. J Cereb Blood Flow Metab 2012;32:1659-76.
13. Suh G-Y, Les AS, Tenforde AS, et al. Hemodynamic changes quantified in abdominal aortic aneurysms with increasing exercise intensity using mr exercise imaging and image-based computational fluid dynamics. Ann Biomed Eng 2011;39:2186-202.
14. Rayz VL, Boussel L, Ge L, et al. Flow residence time and regions of intraluminal thrombus deposition in intracranial aneurysms. Ann Biomed Eng 2010;38:3058-69.
15. Sugiyama SI, Niizuma K, Nakayama T, et al. Relative residence time prolongation in intracranial aneurysms: a possible association with atherosclerosis. Neurosurgery 2013;73:767-76.
16. Hardman D, Doyle BJ, Semple SIK, et al. On the prediction of monocyte deposition in abdominal aortic aneurysms using computational fluid dynamics. J Eng Med 2013;227:1114-24.
17. Kanematsu Y, Kanematsu M, Kurihara C, et al. Critical roles of macrophages in the formation of intracranial aneurysm. Stroke 2011;42:173-8.
18. Cornelissen BMW, Schneiders JJ, Sprengers ME, et al. Aneurysmal parent artery-specific inflow conditions for complete and incomplete circle of Willis configurations. Am J Neuroradiol 2018;39:910-5.
19. Xiang J, Natarajan SK, Tremmel M, et al. Hemodynamic-morphologic discriminants for intracranial aneurysm rupture. Stroke 2011;42:144-52.
20. Doddasomayajula R, Chung B, Hamzei-Sichani F, et al. Differences in hemodynamics and rupture rate of aneurysms at the bifurcation of the basilar and internal carotid arteries. Am J Neuroradiol 2017;38:570-6.
21. Cebral J, Ollikainen E, Chung BJ, et al. Flow conditions in the intracranial aneurysm lumen are associated with inflammation and degenerative changes of the aneurysm wall. Am J Neuroradiol 2017;38:119-26.
22. Cebral XJR, Detmer XF, Chung XBJ, et al. Local hemodynamic conditions associated with focal changes in the intracranial aneurysm wall. Am J Neuroradiol 2019;40:510-6.
23. Epshtein M, Korin N. Mapping the transport kinetics of molecules and particles in idealized intracranial side aneurysms. Nat Sci Rep 2018;8:1-8.
24. Cebral JR, Sheridan M, Putman CM. Hemodynamics and bleb formation in intracranial aneurysms. Am J Neuroradiol 2010;31:304-10.
25. Suzuki T, Takao H, Suzuki T, et al. Determining the presence of thin-walled regions at high-pressure areas in unruptured cerebral aneurysms by using computational fluid dynamics. Neurosurgery 2016;79:589-95.
26. Kleinloog R, Korkmaz E, Zwanenburg JJM, et al. Visualization of the aneurysm wall: a 7.0-Tesla magnetic resonance imaging study. Neurosurgery 2014;75:614-22.
27. Frosen J, Tulamo R, Paetau A, et al. Saccular intracranial aneurysm: pathology and mechanisms. Acta Neuropathol 2012;123:773-86.
28. Baharoglu MI, Lauric A, Gao B-L, et al. Identification of a dichotomy in morphological predictors of rupture status between sidewall- and bifurcation-type intracranial aneurysms. J Neurosurg 2012;116:871-81.
29. Tambasco M, Steinman DA. On assessing the quality of particle tracking through computational fluid dynamic. J Biomech 2002;124:166-75.
30. Závodszky G, Károlyi G, Paál G. Emerging fractal patterns in a real 3D cerebral aneurysm. J Theor Biol 2015;368:95-101.
31. Shadden SC, Arzani A. Lagrangian postprocessing of computational hemodynamics. Ann Biomed Eng 2015;43:41-58.